

# Load Frequency Control of Interconnected Power System with Renewables using Improved Fractional Integral Controller

Kusuma Gottapu\*, Das Prakash Chennamsetty\*\*, Kranthi Kumar Isukapalli\*, Pavan Kumar Gorle \*, Srinivasu Nakka, Durga Prasad Chinta\*

\*Department of Electrical and Electronics Engineering, SRKR Engineering College (A), Bhimavaram, India-534204

\*\* Department of Electrical and Electronics Engineering, GITAM University, Vizag

‡Corresponding Author; Durga Prasad Chinta, SRKR Engineering College, dpchinta@srkrec.edu.in

*Received: 22.10.2022 Accepted: 06.12.2022*

**Abstract-** This article introduces fractional-integral-proportional-derivative (FI-PD) cascade controller as a secondary control scheme of interconnected power system to minimize the frequency and inter area active power disturbances. First, the performance of the FI-PD controller is tested on an interconnected power system with conventional thermal-hydro units, later studies are extended on same test system integrated with wind and solar. To show the improvements achieved with FI-PD controller, classical PI, PID and fractional order PID controllers are opted for comparative assessment. The optimal gains of all the controllers are identified with magnetotactic bacteria optimizer (MBO) algorithm applied first time in automatic generation control. MBO used integral square error as fitness function in the process of identification of optimal gain parameters of the classical and proposed controllers.

**Keywords** Fractional order controller, integral square error, Renewables, magnetotactic bacteria optimizer.

## 1. Introduction

Active power imbalance between generation and demand of an electrical grid initiate the frequency disturbances need to be minimized with the primary and the secondary control mechanisms of the power generating plants. The interconnected power system with traditional generating units have the flexibility to control the power generation in order to meet the demand of utilities [1]. Classical controllers are available as secondary controllers in conventional power system models to meet the objectives of the AGC [2]. With integration of renewables, power generation varies along with the demand causes the frequency deviations and superior controllers are required to minimize the deviations [3]. In recent times, several research findings are available in the literature on AGC of interconnected power system models integrated with high renewable power penetration [4]-[14]. Studies are also available in isolated and coupled scenarios of power system in presence of wind and solar distribution generation (DG) units [15]-[18]. To find the optimal gains of

the controllers to achieve the goals of AGC of modern power systems including renewables, heuristic algorithms are useful similar to conventional studies. For example, whale optimization algorithm is used in [4] to tune PID controller of the secondary control loop of renewable integrated modern power system. In conventional power system, generation is continuously controlled during normal operating conditions and energy storage systems are required when it is integrated with renewables due to their volatile nature and availability. In [5], AGC of wind park is presented with energy storage to show the impact of ES in frequency control. In case of high penetration of wind energy, distributed generation control approaches are better compared to regular AGC. A flatness-based control is proposed in [6] to control the frequency of the multi area power system. In [7], another optimal control mechanism is presented on a 2-area system with thermal, hydro, and gas-based conventional generations along with wind power. The main concern of these renewables is to reduce the environmental pollution generated by conventional generation resources. Electric vehicles (EV) is another section

to address the same benefits. Few AGC studies are available in literature of AGC on both wind, solar and EV. In [8], such study is available with wind and EV on AGC of the modern power system. Other scenarios are also tested in earlier research studies [9]-[14]. In [9], deregulated multi area power system is considered to study the impact of the solar generation on AGC with optimal cascade controller. The gains are achieved with differential evolution (DE) algorithm. In [10], FACT device is included in the power system with renewables to study the frequency control aspects and a multistage controller tuned by particle swarm optimizer (PSO) is used in AGC to minimize the frequency deviations of the power system. In [11], both wind and solar units are considered with large capacities to study their impact of frequency control with PI and PID controllers. Apart from the optimization assisted classical and modern controllers, few intelligent controllers were tested. In [12], fuzzy logic (FL)-based controller is proposed to minimize the frequency deviations of the power system integrated with high penetration of wind. The response is superior to classical PI and PID controllers. To use these models in AGC, modelling is available in [13]. The participation of wind in different scenarios of power system are also available in literature. In [14]-[15], interconnected power system scenario is considered to study the frequency stability issues during load perturbations in presence of renewables. Distribution generation (DG) by wind and solar in small scale is used in microgrids and AGC studies on microgrids are available in [16]-[19]. In [16], stochastic non-integer controller is proposed to minimize the frequency oscillations of the microgrid. In [17], frequency control of microgrid with EV is proposed with PSO-based artificial neural networks. In [18], multi and islanded AC microgrid models are considered to study the AGC. Another important factor in these renewable integrated system is forecasting [19]. Recently forecasting based models are implemented in AGC to coordinate demand and generation [19]. The cascade fractional controllers related works are also popular due to their significant improvements in the performance of the AGC studies in presence of storage units [20]. Combined controller schemes are also available in literature to meet the goals of the AGC during load disturbances [21]. Apart from the controller novelties, tuning algorithms modifications are also provided enhanced outputs due to their efficiency in identifying the optimal parameter gains of the controllers [22]. These advancements in AGC schemes improve the system stability during load and generation uncertainties [23]. Still challenges are alive due to integration of renewables in different stages.

In this paper, a new fractional integral-proportional-derivative (FI-PD) cascade controller is proposed to reach the goals of AGC of multi area multi machine interconnected power system integrating with both solar and wind. The optimal gain of the controller is obtained with magnetotactic bacteria optimize (MBO) [24]-[26] with the help of integral square error (ISE) as cost function. Investigations are carried out with and without integration of wind and solar and comparisons are performed with PI, PID and FOPID controllers. Additionally, comparisons are provided with PSO, DE and IWO to show the merits of the MBO in AGC studies.

Simulations are carried out in MATLAB SIMULINK and paper organizes as follows: Section 2 includes combined details of the test system and proposed controller. Section 3 include fitness function and tuning algorithm. Section 4 presents simulation results and conclusions are provided in Section 5.

## 2. Test System with Proposed Controller

Multi area interconnected power system integrated with wind and solar in one area is opted in this paper to study the effect of the proposed controller along with existing classical and FO controllers on AGC [27]-[29]. The simple average demand variations, generation changes, noise in renewables and parameters uncertainties are simulated to test the frequency profile enhancement with the proposed controller. The details of the test system and the controller are provided in the below sub sections.

### 2.1. Overview of the Test System

Fig. 1 shows the block diagram of the AGC assisted 2-area interconnected power system model. In each area, both thermal and hydro plants are included with ideal components. These conventional power generating plants have both primary and secondary control loops to regulate their power generations. Additionally, wind and solar units are integrated in area 1 and the power generation from these renewable sources are independent and volatile in nature. Therefore, generation changes are appeared in the system along with load perturbations especially in the area 1. The parameters of the test system are provided in appendix 1.

### 2.2. Proposed Controller

To improve the frequency profiles, FI-PD cascade controller is used as secondary control mechanism of the interconnected power system. The schematic diagram of the proposed controller is presented in Fig. 2. The controller consists of two sub blocks known as fractional integral component and PD component. This controller utilizes both change in frequency and area control error (ACE) to produce necessary control action. De-centralized control mechanism is used in the AGC architecture which produces control signals to all the participating units of the corresponding area. This AGC mechanism is included in Fig. 1. The control input of the individual plants of the test system by the proposed FI-PD controller is provided in Equation (1).

$$u_i(s) = \left( \Delta f_i(s) - ACE_i(s) \left( \frac{k_{ii}}{s^{\alpha_i}} \right) \right) (k_{p_i} + k_{d_i}s) \quad (1)$$

In Equation (1),  $k_{p_i}$ ,  $k_{i_i}$ ,  $k_{d_i}$  and  $\alpha_i$  are the optimal parameter gains of the proposed controller individually represented by the proportional, integral, derivative, and fractional gains. Since the test system consists of 4 conventional plants and therefore 4 controllers are needed with 16 parameter gains. All these gains are identified by using MBO algorithm with the help of ISE fitness function.

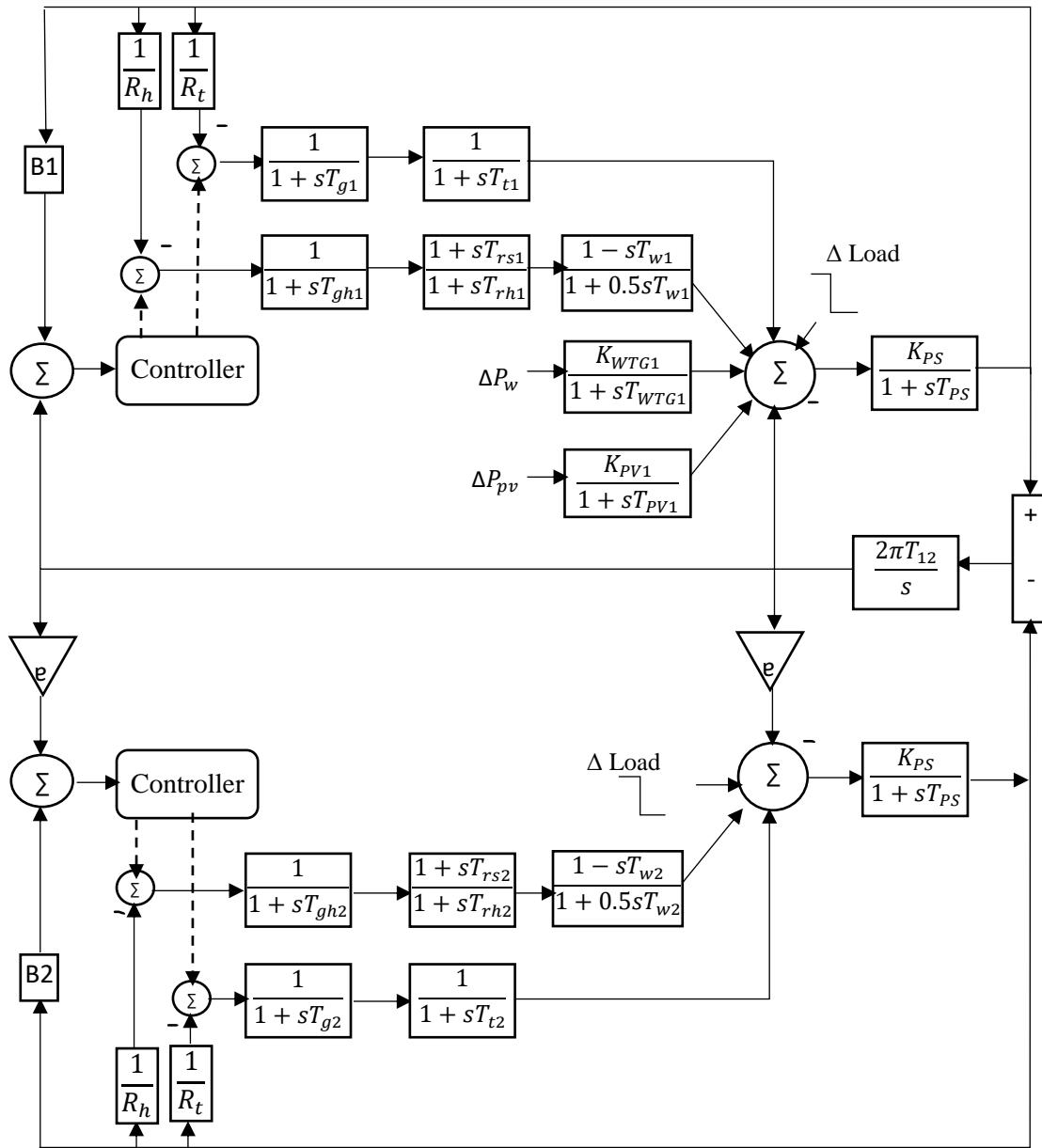


Fig. 1. Test system block diagram

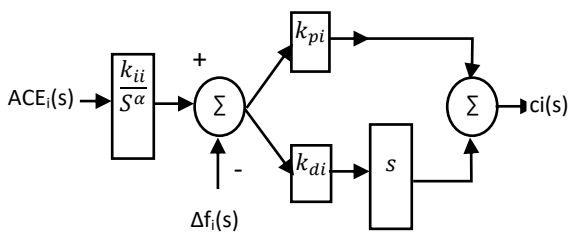


Fig. 2. Structure of the proposed controller

### 3. Fitness Function and Tuning Algorithm

To set the controllers optimal gain parameters using meta-heuristic algorithms, proper fitness/cost function is necessary. ISE is the popularly used cost function in AGC studies and it is expressed as

$$ISE = \int_0^t \sum \{(\Delta f_i)^2 + (\Delta P_{ij})^2\} dt \quad (2)$$

In Equation (2),  $\Delta f_i$  is the change in frequency of  $i^{th}$  area and  $\Delta P_{ij}$  is the active power carried by the tie-line connected in between the areas  $i$  and  $j$ . Based on selection of optimal parameter gains of the controllers, the value of the fitness function changes and these gains are generated by MBO to minimize the frequency disturbances of the test system. The details of MBO are available in [24]-[26]. This algorithm is designed with magnetotactic bacteria behavior in similar way of other meta-heuristic algorithms with initialization, power spectrum calculation, bacteria rotation, and replacement computational steps. Solutions are randomly generated in the initialization of optimization process provided within the boundaries of the decision variables using the Equation (3)

$$x_{i,j} = x_{min,j} + rand * (x_{max,j} - x_{min,j}) \quad (3)$$

The random number generated in between 0 and 1 is denoted by  $rand$  in the Equation (3).  $x_{max,j}$  is the maximum value and  $x_{min,j}$  is the minimum value of the  $x$ . To generate the new solution in the process of the optimal solution search, two bacteria particles are selected randomly  $x_{r1,j}$  and  $x_{r2,j}$  with the difference given by

$$L_{r1,r2}^t = x_{r1,j}^t - x_{r2,j}^t \quad (4)$$

In Equation (4),  $t$  is iteration number. Further, the power spectrum of a single bacteria  $S_i$  is identified with Equation (5) to update the solution for the next iteration using Equation (6)

$$S_{i,j}^t = \frac{2\tau_{p,q}^t}{1+(2\pi f\tau_{i,j}^t)^2} \quad (5)$$

$$x_{i,q}^{t+1} = x_{p,q}^t + S_{i,j}^t \quad (6)$$

After rotation, the bacteria swim as follows:

$$x_i^{t+1} = \left. \begin{aligned} &x_{best}^t + rand * (x_{best}^t - x_i^t), \text{ if } rand > 0.5 \\ &x_i^t + rand * (x_{best}^t - x_i^t), \text{ otherwise} \end{aligned} \right\} \quad (7)$$

For more convergent outputs, few worst solutions are replaced by using Equation (8)

$$x_i^{t+1} = S_{p,q}^t * ((rand(1,n) - 1) * rand(1,n)) \quad (8)$$

In the updating mechanism of the MBO, power spectrum calculation, bacteria rotation, and replacement computational steps are repeated to generate new solutions until maximum iterations are attained. In MBO, each bacteria particle represents controller parameter gain and optimal gains are achieved at the end of the iterations of the MBO.

#### 4. Simulation Results

The performance of the proposed controller is tested on renewable penetrated power system shown in Fig. 1 at different loadings, generation changes and the parameters uncertainties. In each investigation, comparisons are provided with PI, PID and FOPID controllers tuned by MBO algorithms with ISE measure. All these investigations are simulated at optimal gains of the controllers reported in Table 1 produced using MBO algorithm.

##### 4.1 Simple Load Perturbations (SLP)

A load change of 0.01 p.u is initiated in the area 1 by neglecting the renewable generations as well as load variations in other areas. Fig. 3 shows the changes in area 1 frequency corresponding to the load changes in presence of both primary and secondary control loops. Tie-line power disturbances in between the interconnected areas are provided in Fig. 4 followed by Fig.5 with area 2 frequency changes. The change in load is negative (decrease) and system frequency increases from its nominal value and therefore change in frequency is also negative. This is evident from the Fig. 3 and Fig 5. Further, a positive load change is initiated in the area 1 with a quantity of 0.05 and changes in area 1 frequency deviations are reported in Fig. 6. Tie-line power disturbances in between the interconnected areas are provided in Fig. 7 followed by Fig.8 shows area 2 frequency deviations when a SLP of 5% is initiated in the area 1 at time 0 sec. The frequency disturbances

of both areas are positive since the demand is increased in the area 1.

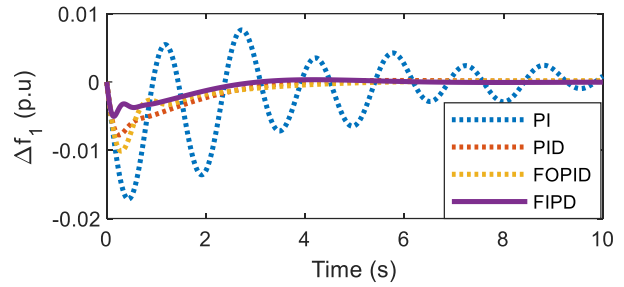


Fig. 3. Area 1 frequency deviations for SLP of 1% in area 1

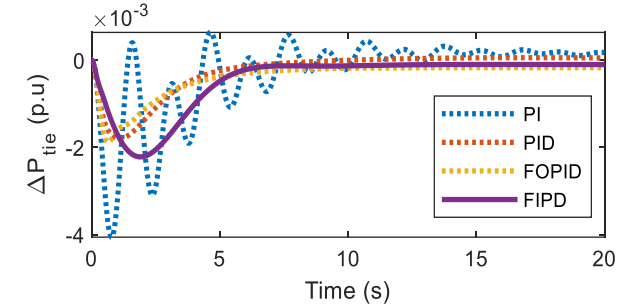


Fig. 4. Tie-line power deviations under SLP of 1% in area 1

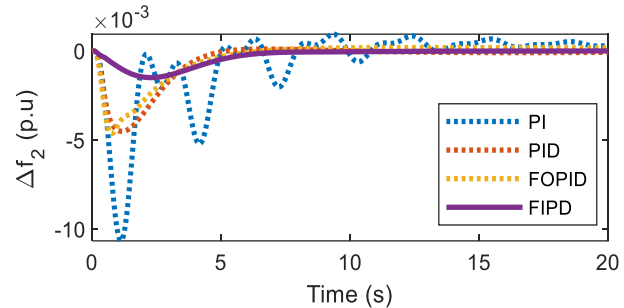


Fig. 5. Area 2 frequency deviations for SLP of 1% in area 1

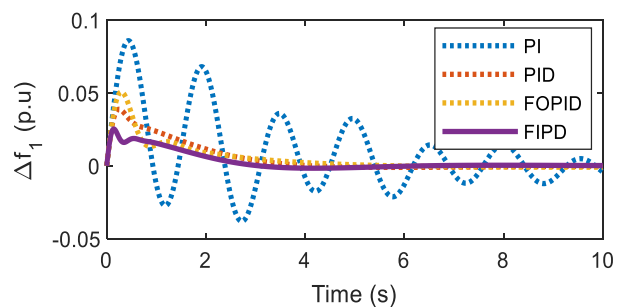


Fig. 6. Area 1 frequency deviations for SLP of 5% in area 1

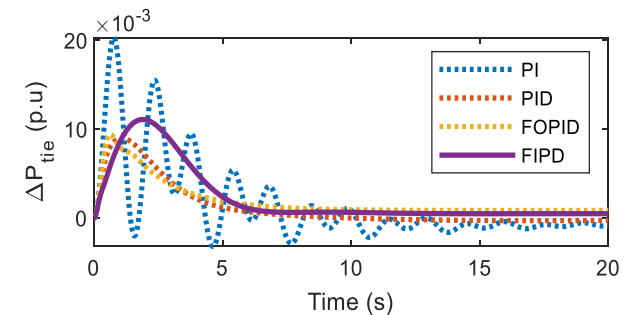
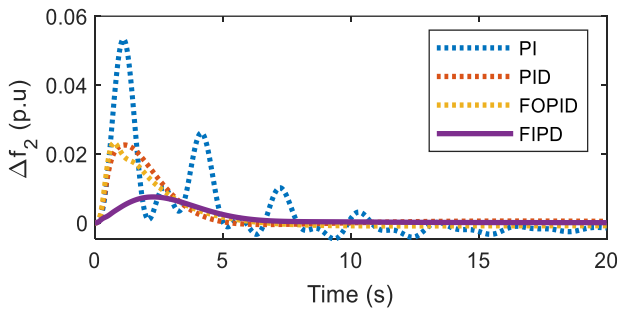


Fig. 7. Tie-line power deviations under SLP of 5% in area 1

**Table 1.** Optimal parameter gains of the controllers using MBO

Area and Machine	Parameter	PI	PID	FOPID	FIPD
Area-1	$k_p$	-0.9968	-0.9993	-1	-0.9987
Machine-1	$k_i$	-0.5046	-1	-0.9786	-0.9979
	$k_d$	--	-1	-0.9898	-1
	$\alpha$	--	--	-0.9898	-1
	$\beta$	--	--	0.6925	--
	$k_p$	1	-0.6985	-0.9796	1
Machine-2	$k_i$	-1	0.1445	-0.9987	0.9418
	$k_d$	--	0.1259	0.8364	-0.9849
	$\alpha$	--	--	-0.0110	0
	$\beta$	--	--	0.9569	--
	$k_p$	0.3926	0.4162	-0.3318	-1
Machine-1	$k_i$	-0.7531	-0.0365	0.9357	-0.0639
	$k_d$	--	-0.7606	-0.9335	-1
	$\alpha$	--	--	0	-0.3605
	$\beta$	--	--	1	--
	$k_p$	-0.6245	0.1779	0.7253	-0.9479
Machine-2	$k_i$	-0.3853	-0.5279	0.9726	0.8118
	$k_d$	--	-0.7486	-1	-0.9868
	$\alpha$	--	--	0	-0.2126
	$\beta$	--	--	0	-0.2126
	$k_p$	-0.9968	-0.9993	-1	-0.9987



**Fig. 8.** Area 2 frequency deviations for SLP of 5% in area 1

In both loadings, the performance of the proposed FI-PD controllers is good compared to other controllers. The peak overshoot, settling time and ISE values are reduced drastically compared to PI, PID and FOPID controllers.

**4.2 Generation Changes (GC) in Wind and Solar Units**

To investigate AGC studies corresponding to the variations of the inputs of wind and solar, generation changes are considered in this case study. For this purpose, generation changes of (change in wind and solar power) renewables are simulated at 0 sec with magnitude of 0.01 p.u. in area 1 by maintaining all the input changes of area 2 as zero along with the load perturbations of area 1 and area 2. Compared to other controllers, proposed FI-PD controller yields superior performance during the load and generation perturbations as shown in Fig. 9, Fig. 10, and Fig. 11. In detail, frequency changes of area 1 are reported in Fig. 9, tie-line power deviations in Fig. 10 and area 2 frequency variations in Fig. 11.

**4.3 Diverse Generation Changes (DGC)**

The generation changes are random in nature due to intermittency nature of the PV and wind inputs. Such changes are simulated in the system as shown in Fig. 12. In this case different input changes are initiated for wind and solar units integrated in area 1 and responses are provided in Fig. 13, Fig. 14, and Fig. 15. One GC is simulated at 0 sec and second GC is considered at 20 sec. Under DGC, the FI-PD controller performance is competent compared to classical and fractional order controller. The noise in the generation is also included in the simulation studies to incorporate the intermittency nature of the wind and solar inputs. In such environment, the proposed controller provided better results compared to other classical controllers along with the fractional order controller. Therefore, it is observed that the proposed controller is suitable in such DGC scenarios.

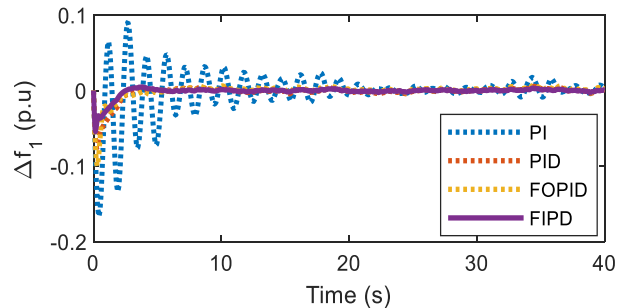


**Fig. 9.** Area 1 frequency deviations for GC of 1% in area 1

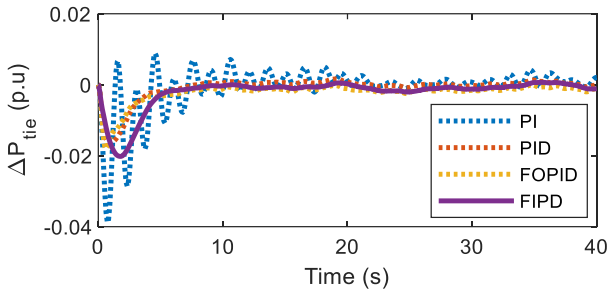


**Fig. 10.** Tie-line power deviations under GC of 1% in area 1

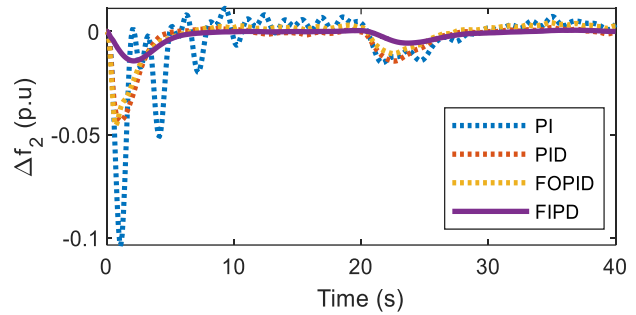


**Fig. 15.** Area 2 frequency deviations under DGC of 1% and 5% in area 1

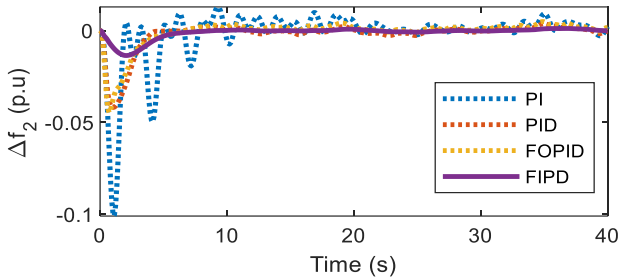


**Fig. 11.** Area 2 frequency deviations for GC of 1% in area 1

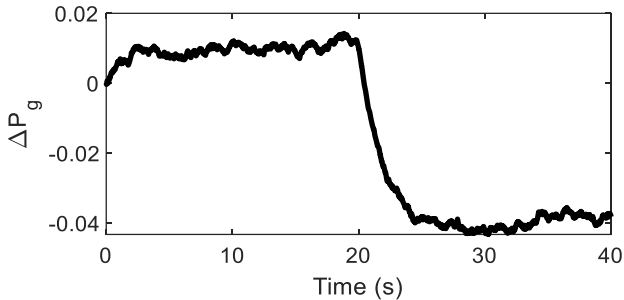


**Fig. 12.** The pattern of GC and DGC simulation outputs

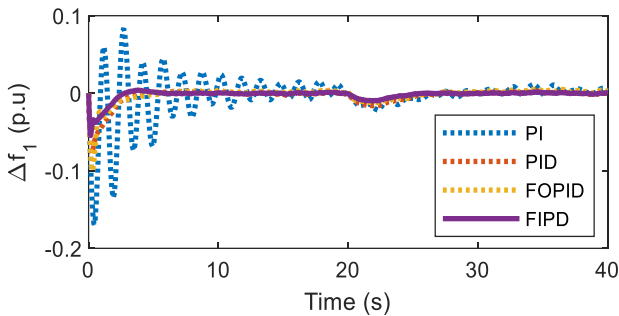


**Fig. 13.** Area 1 frequency deviations for DGC of 1% and 5% in area 1

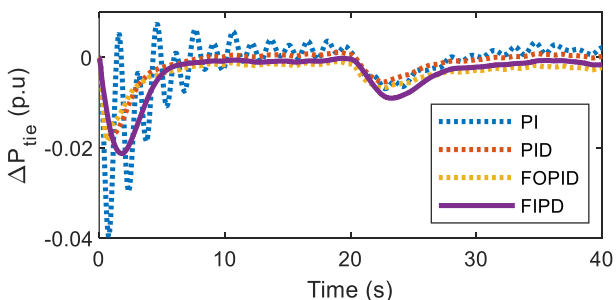


**Fig. 14.** Tie-line power deviations under DGC of 1% and 5% in area 1

**4.4 Load-Generation Simultaneous Changes (LGSC)**

A Load disturbance of 10% and a GC of 5% from both wind and solar is used in this case study to check the effectiveness of the proposed controller and comparisons are performed with PI, PID and FOPID controllers. Fig. 16, Fig. 17, and Fig. 18 shows the area 1 frequency, tie-line power and area 2 frequency deviations from its nominal value. In each plot, the response of the proposed controller is good compared to the other controllers and quick frequency stability is achieved in the system during load and generation changes with the proposed controller.

**4.5 Parameter Sensitivities**

All the controller gains are identified using MBO at constant system parameters. In practical situations, the system parameters alter based on the dynamic conditions. To check the effectiveness of the proposed controller, sensitivity analysis is carried out on the test system for one typical power system gain parameter. During the regular cases, the value of the power system gain is 120 and evaluated the performance of the proposed controller at 100 using the same optimal gains achieved for original system. Both responses are plotted from the Fig. 19 to Fig. 21. In Fig. 19, frequency deviations of the area 1 are plotted. In Fig. 20, tie-line power deviations of the areas 1-2 are presented. In Fig. 21, frequency deviations of the area 2 are plotted. From these Figures, it is evident that the proposed controller minimized the impact of the parameter variations on frequency and tie-line disturbances. Similar to load damping variations, other factors variations are also minimum on system performance.

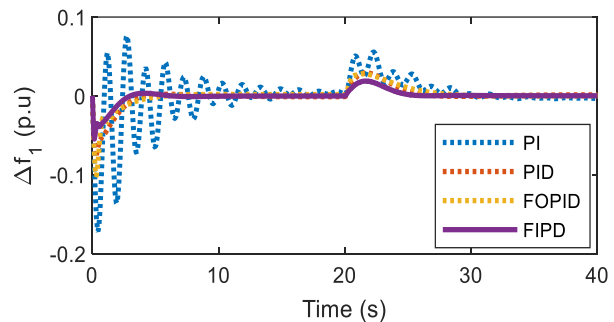


**Fig. 16.** Area 1 frequency deviations under LGSC.

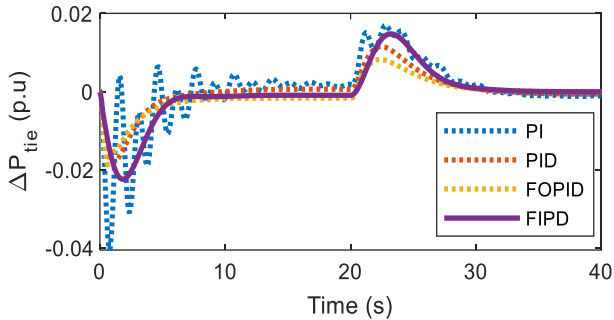


Fig. 17. Tie-line power deviations under LGSC

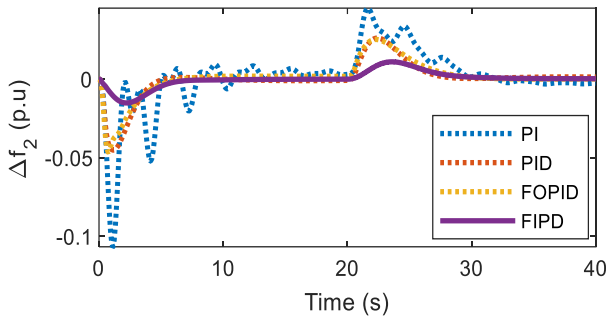


Fig. 18. Area 2 frequency deviations under LGSC

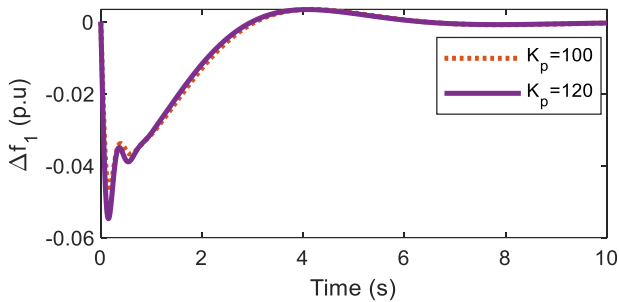


Fig. 19. Area 1 frequency deviations with parameter changes

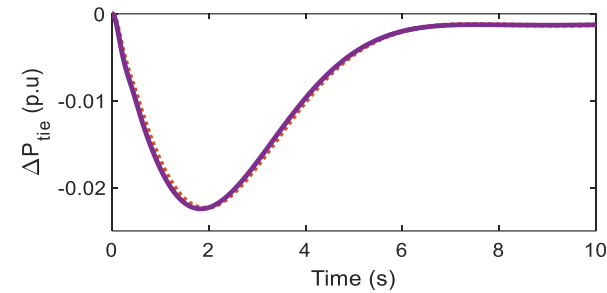


Fig. 20. Tie-line power deviations with parameter changes

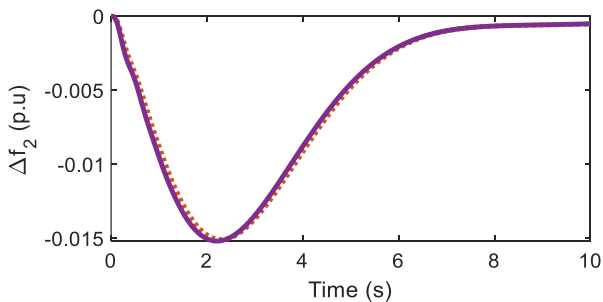


Fig. 21. Area 2 frequency deviations with parameter changes

#### 4.6 Comparative Assessment

The optimal gains of the controllers are obtained using MBO and comparisons are provided with PSO [], DE [] and IWO [] to show the improvements. Fig. 22 shows the comparisons of the area-1 frequency deviations with proposed controller assisted with optimized gains. The MBO associated system results are provided good performance compared to other systems.

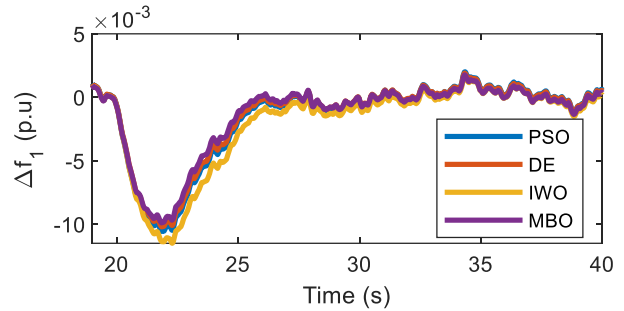


Fig. 22. Area 1 frequency deviations with different tuning algorithms.

#### 5. Conclusion

This article suggested FI-PD controller to minimize the frequency disturbances of interconnected power system integrating with wind and solar power generations. The proposed controller produces better results compared to classical PI, PID and FOPID controllers in case of simple load perturbations, generation changes and load and generation simultaneous variations. Sensitivity analysis carried out on the test system provided the effectiveness of the proposed controller. The MBO algorithm provided acceptable results compared to PSO, DE and IWO in terms of the performance specifications.

#### Appendix

##### System Parameters:

Thermal plant:  $T_g=0.08$ ;  $T_t=0.3$ ;  $R_t=2.4$ , Hydro plant:  $T_{gh}=48.7$ ;  $T_{rs}=5$ ;  $T_{rh}=0.513$ ;  $T_w=1$ ;  $R_h=2.4$ , Wind and Solar:  $K_{WTG}=1$ ;  $T_{WTG}=1.5$ ;  $K_{PV}=1$ ;  $T_{PV}=1.8$ , Power system:  $K_{PS}=120$ ;  $T_{PS}=20$ ;  $B_1=B_2=0.425$ ;  $2\pi T_{12}=0.545$

#### References

- [1] P. Kumar, and D.P. Kothari, "Recent philosophies of automatic generation control strategies in power systems", *IEEE transactions on power systems*, vo.; 20, no. 1, pp.346-357, 2005.
- [2] L.C. Saikia, J. Nanda, and S. Mishra, "Performance comparison of several classical controllers in AGC for multi-area interconnected thermal system", *International Journal of Electrical Power & Energy Systems*, vol. 33, no. 3, pp.394-401, 2011.
- [3] M. Ramesh, A.K. Yadav, and P.K. Pathak, "An extensive review on load frequency control of solar-wind based

- hybrid renewable energy systems", *Energy Sources, Part A: Recovery, Utilization, and Environmental Effects*, pp.1-25, 2021.
- [4] H.M. Hasanien, "Whale optimisation algorithm for automatic generation control of interconnected modern power systems including renewable energy sources", *IET Generation, Transmission & Distribution*, vol. 12, no. 3, pp.607-614, 2018.
- [5] T. Chakraborty, D. Watson, and M. Rodgers, "Automatic generation control using an energy storage system in a wind park", *IEEE Transactions on Power Systems*, vol. 33, no. 1, pp.198-205, 2017.
- [6] M.H. Variani, and K. Tomsovic, "Distributed automatic generation control using flatness-based approach for high penetration of wind generation", *IEEE Transactions on Power Systems*, vol. 28, no. 3, pp.3002-3009, 2013.
- [7] N. Hakimuddin, I. Nasiruddin, T.S. Bhatti, and Y. Arya, "Optimal automatic generation control with hydro, thermal, gas, and wind power plants in 2-area interconnected power system", *Electric Power Components and Systems*, vol.48, no. 6-7, pp.558-571, 2020.
- [8] K. Ullah, A. Basit, Z. Ullah, F. R. Albogamy, and G. Hafeez, "Automatic Generation Control in Modern Power Systems with Wind Power and Electric Vehicles", *Energies*, vol.15, no. 5, pp.1771, 2022.
- [9] G. P. Kumar, R. Srinu Naik, and C.D. Prasad, "Application of the PI-PD cascade control scheme in AGC of a deregulated power system with PV in the presence of communication delay", *International Journal of Ambient Energy*, 2021.
- [10] N.K. Jena, N.C. Patel, S. Sahoo, B.K. Sahu, S.S. Dash, K.B. Mohanty, and R. Bayindir, "Novel application of Selfish Herd Optimisation based Two Degrees of Freedom Cascaded Controller for AGC Study." *2019 8th International Conference on Renewable Energy Research and Applications (ICRERA)*. IEEE, 2019.
- [11] K. Kiran Kumar, G. Balaji, P.Kanta Rao, and C.D. Prasad, "Frequency Control of Isolated Power System Integrated with Renewables using Biogeography based Krill Herd Migration Optimized Controllers", *International Journal of Renewable Energy Research*, vol. 12, no. 1, pp. 529-535, 2022.
- [12] H. Bevrani, and P.R.Daneshmand, "Fuzzy logic-based load-frequency control concerning high penetration of wind turbines", *IEEE systems journal*, vol. 6, no. 1, pp.173-180, 2011.
- [13] Chang-Chien, Le-Ren, C.C.Sun, and Y.J.Yeh, "Modeling of wind farm participation in AGC", *IEEE Transactions on Power Systems*, vol. 29, no. 3, pp.1204-1211, 2013.
- [14] B. Vedik, R. Kumar, R. Deshmukh, S. Verma, and C.K.Shiva, "Renewable energy-based load frequency stabilization of interconnected power systems using quasi-oppositional dragonfly algorithm", *Journal of Control, Automation and Electrical Systems*, vol. 32, no. 1, pp.227-243, 2021.
- [15] D.H. Tungadio, and Y.Sun, "Load frequency controllers considering renewable energy integration in power system", *Energy Reports*, vol. 5, pp.436-453, 2019.
- [16] M.H. Khooban, T. Niknam, M. Shasadeghi, T.Dragicevic, and F.Blaabjerg, "Load frequency control in microgrids based on a stochastic noninteger controller." *IEEE Transactions on Sustainable Energy*, vol. 9, no. 2, pp.853-861, 2017.
- [17] A. Safari, F. Babaei, and M. Farrokhifar, "A load frequency control using a PSO-based ANN for micro-grids in the presence of electric vehicles", *International Journal of Ambient Energy*, vol. 42, no. 6, pp. 688-700, 2021.
- [18] P.C. Sahu, S.Mishra, R.C.Prusty, and S.Panda, "Improved-salp swarm optimized type-II fuzzy controller in load frequency control of multi area islanded AC microgrid", *Sustainable Energy, Grids and Networks*, vol.16, pp.380-392, 2018.
- [19] D. Kumar, H. D. Mathur, S. Bhanot, and R.C.Bansal, "Forecasting of solar and wind power using LSTM RNN for load frequency control in isolated microgrid", *International Journal of Modelling and Simulation*, vol. 41, no. 4, pp. 311-323, 2021.
- [20] R. Choudhary, J. N. Rai, and Y. Arya, "Cascade FOPI-FOPTID controller with energy storage devices for AGC performance advancement of electric power systems", *Sustainable Energy Technologies and Assessments*, vol. 53, pp. 102671, 2022.
- [21] M. Azaharahmed, K. Raja, M. Patan, C.D. Prasad, and P. Ganeshan, "Invasive weed optimized area centralized 2 degree of freedom combined PID controller scheme for automatic generation control", *Journal of Electrical Engineering & Technology*, vol. 16, no. 1, pp. 31-42, 2021.
- [22] B. Khokhar, S. Dahiya, and KP Singh Parmar, "Load frequency control of a microgrid employing a 2D Sine Logistic map based chaotic sine cosine algorithm", *Applied Soft Computing*, vol. 109, pp.107564, 2021.
- [23] E. Sri Lalitha, A. M. S. V. Sushma, G.P. Kumar, and C.D. Prasad, "Biogeography-Based Centralized PID Controller for ALFC in Presence of Wind Farms", In *Recent Advances in Manufacturing, Automation, Design and Energy Technologies*, pp. 853-858, 2022.
- [24] M. Hongwei, "Research on magnetotactic bacteria optimization algorithm." In *2012 IEEE Fifth International Conference on Advanced Computational Intelligence (ICACI)*, pp. 423-427, 2012.
- [25] M. Hongwei, L. Liu, and L. Xu, "A power spectrum optimization algorithm inspired by magnetotactic bacteria", *Neural Computing and Applications*, vol.25, no.7, pp.1823-1844, 2014.
- [26] M. Hongwei, L. Liu, and J. Zhao, "A new magnetotactic bacteria optimization algorithm based on moment

migration", *IEEE/ACM transactions on computational biology and bioinformatics*, vol.14, 1, pp.15-26, 2015.

- [27] S. Janković and B. Ivanović, "Real Life Permissive LFC Model Description," *2018 IEEE PES Innovative Smart Grid Technologies Conference Europe (ISGT-Europe)*, pp. 1-6, 2018.
- [28] S. J. Gambhire, M. K. Kumar, K. Mallikarjuna, A. N. Venkateswarlu, C. N. Sai Kalyan and B. S. Goud, "Performance Comparison of Various Classical Controllers in LFC of Hydro-Thermal Power System with Time Delays," *2022 10th International Conference on Smart Grid (icSmartGrid)*, pp. 401-406, 2022.
- [29] M. O. Abdul Kader, K. T. Akindeji and G. Sharma, "Application of PHEVs Influence on Frequency Regulation of a Two Area Power System," *2022 10th International Conference on Smart Grid (icSmartGrid)*, pp. 23-28, 2022.